# Optimal Control of Vortex Shedding Using Low Order Models
# Part II: Model-Based Control

By **W. R. GRAHAM**[1] , **J. PERAIRE**[2] AND **K. Y. TANG** [2]

[1]Department of Engineering, University of Cambridge, Cambridge, England
[2]Department of Aeronautics and Astronautics, Massachusetts Institute of Technology, Cambridge, Ma 02129, U.S.A

(Received 5 December 1997)

In Part I, an approach to deriving low order models suitable for use in the development of active control strategies for separated flows was presented. The methodology proposed was applied to a numerical simulation of the incompressible, unsteady wake flow behind a circular cylinder at Re = 100, with control action achieved via cylinder rotation. The resulting low order models were found to predict the flows in four open-loop test cases with sufficient fidelity to justify their application in model-based control of the vortex-shedding flow. In Part II, optimal control theory is used to implement the model-based control, and data from numerical simulations of the controlled flow are presented. It is found that the level of wake unsteadiness can be reduced, even when the low order model is reset on the basis of limited flow field information. The degree of reduction is dependent on the accuracy of the low order model, and ways of refining it in the light of control simulations are considered. However, results from two straightforward approaches to this problem suggest that it is easy to "over-tune" the model, resulting in less successful control.

## 1. Introduction

In Part I of this work, the Proper Orthogonal Decomposition (POD) approach to generating low order models for the flow about a circular cylinder was extended to allow the incorporation of control action, in this case cylinder rotation, and its effect on the flow. The resulting low order models were shown to be capable of describing control-induced departures from steady state conditions with far greater success than models derived from the standard POD approach, making it feasible to envisage employing them for model-based control of the vortex-shedding flow. In this paper we describe investigations into this approach.

Given the form of our low order models, with flow velocities represented in terms of the mean flow and a sum of "modes" (POD basis functions), a natural control aim is the reduction of the wake unsteadiness, associated with the mode amplitudes. In the light of the introductory discussion in Part I, we cannot expect to suppress the unsteadiness entirely, but we can hope to reduce it. We also note from Part I that cylinder rotation tends, in general, to increase the level of wake unsteadiness, (the most extreme manifestation being locked-on flow), so that achieving reductions via this approach will be a clear demonstration of the success of the control method.

The first requirement here is a suitable formulation for the model-based control, and in section 2 we describe such a formulation, based on optimal control ideas (Lions 1971, Pironneau 1984). This formulation depends on whether the low order model chosen arises from the penalty method or the control function method, and both versions are presented here. The application of the formulation to model-based control of our numerical simulation is then discussed in section 3. Since the low order model has a limited "look-ahead" time over which its predictions are valid, the control here assumes the ability to reset the model periodically, and the results therefore represent an idealized performance. A significant issue is the sensitivity of the control performance to the basis functions used in the low order model, and in section 4 we discuss methods for improving the basis functions. The other important question is the extent to which the control performance is degraded by resetting the model on the basis of only limited information, as would be necessary in a more realistic scenario, and this is addressed in section 5.

## 2. Optimal Control Formulations

In this section we discuss the formulation of our problem in optimal control terms. Here the aim is to minimize a cost function, which incorporates the control goal and some measure of the control effort, over a certain period of time. Clearly, in order to find the necessary control one must be able to predict the system behavior during this period, hence the importance of developing accurate low order models. Given such a model, the optimal control problem may then be efficiently formulated and solved.

The details of this approach inevitably depend on the form of the low order model, and we must thus derive two formulations, one for the penalty method (presented first, in section 2.1, due to its greater simplicity) and one for the control function method (discussed in section 2.2). The results of the two approaches are then compared for a test example in section 2.3.

### 2.1. *Penalty Method Formulation*

We define a cost function

$$E = \int_0^T e(\mathbf{y}, \gamma) dt \tag{2.1}$$

where $e(\mathbf{y}, \gamma)$ reflects our control aims and expense. Here we associate our desire to reduce the wake unsteadiness with the mode amplitudes, $y_i$, and take

$$e(\mathbf{y}, \gamma) = \sum_{i=1}^{N} y_i^2 + e^{C(\gamma^2 - \gamma_{max}^2)} \tag{2.2}$$

where the second term, with $C$ large and positive, imposes a severe cost on any control amplitudes $\gamma > \gamma_{max}$.

We wish to minimize $E$ subject to the constraint that the $y_i$s and $\gamma$ obey the low order model derived in Part I:

$$\frac{dy_i}{dt} = a_i^p + \sum_{j=1}^{N} b_{ij}^p y_j + \sum_{j=1}^{N} \sum_{k=1}^{N} c_{ijk} y_j y_k + d_i^p \gamma. \tag{2.3}$$

This constraint may be included in the minimization problem by introducing adjoint functions $\theta_i(t)$ and writing

$$E = \int_0^T e(\mathbf{y},\gamma)dt - \int_0^T \sum_{i=1}^N \theta_i(\frac{dy_i}{dt} - a_i^p - \sum_{j=1}^N b_{ij}^p y_j - \sum_{j=1}^N \sum_{k=1}^N c_{ijk} y_j y_k - d_i^p \gamma)dt \quad (2.4)$$

On taking variations, and integrating by parts, we have

$$\delta E = \int_0^T \sum_{i=1}^N (\frac{\partial e}{\partial y_i} + \frac{d\theta_i}{dt} + \sum_{j=1}^N [b_{ji}^p + \sum_{k=1}^N (c_{jki} + c_{jik}) y_k]\theta_j)\delta y_i dt$$
$$-[\sum_{i=1}^N \theta_i \delta y_i]_0^T + \int_0^T (\frac{\partial e}{\partial \gamma} + \sum_{i=1}^N d_i^p \theta_i)\delta\gamma dt \quad (2.5)$$

where the admissible variations $\delta y_i$ have $\delta y_i(0) = 0$ (initial condition fixed). Thus, if we define the adjoint functions $\theta_i$ by the requirements

$$\theta_i(T) = 0 \quad (2.6)$$

$$\frac{d\theta_i}{dt} = -\sum_{j=1}^N [b_{ji}^p + \sum_{k=1}^N (c_{jki} + c_{jik}) y_k]\theta_j - \frac{\partial e}{\partial y_i} \quad (2.7)$$

the variation takes the simple form

$$\delta E = \int_0^T (\frac{\partial e}{\partial \gamma} + \sum_{i=1}^N d_i^p \theta_i)\delta\gamma dt \quad (2.8)$$

Given a set of initial conditions, $y_i(0)$, and an initial control $\gamma(t)$, we may evaluate the bracketed term in equation (2.8) by first using equation (2.3) to integrate forwards for the $y_i$, and then equations (2.6), and (2.7) to integrate backwards for the $\theta_i$. Modification of the control by the steepest descent choice

$$\delta\gamma = -\Delta_s(\frac{\partial e}{\partial \gamma} + \sum_{i=1}^N d_i^p \theta_i) \quad (2.9)$$

then ensures, for a sufficiently small step size $\Delta_s$, that $E$ is reduced. As $\Delta_s$ is increased $\delta E$ will become positive, and an optimum value must be found using a line search. The associated $y_i$s and $\gamma(t)$ then form the initial condition for another steepest descent step.

As presented above, this formulation places no restrictions on $\delta\gamma$, a feature which leads to a jump discontinuity in $\gamma$ at $t = 0$. The requirement that $\gamma$ should, in fact, vary smoothly is found to be best implemented via a parametrization:

$$\gamma(t) = \gamma(0)[1 - \frac{t}{T}] + \sum_{m=1}^M \gamma_m sin(\frac{m\pi t}{2T}) \quad (2.10)$$

The variation in $\gamma$ parametrized in this way is

$$\delta\gamma = \sum_{m=1}^{M} \delta\gamma_m sin(\frac{m\pi t}{2T}) \tag{2.11}$$

and the steepest descent "direction" is now given by

$$\delta\gamma_m = -\Delta_s \int_0^T (\frac{\partial e}{\partial \gamma} + \sum_{i=1}^{N} d_i^p \theta_i) sin(\frac{m\pi t}{2T}) dt \tag{2.12}$$

## 2.2. *Control Function Method Formulation*

Since the velocity expansion in this method takes the form

$$\mathbf{u}(\mathbf{x}, t) = \mathbf{u}_m(\mathbf{x}) + \gamma \mathbf{u}_c(\mathbf{x}) + \sum_{i=1}^{N} y_i \mathbf{\Psi}_i(\mathbf{x}) \tag{2.13}$$

(equation (4.2) of Part I), the wake unsteadiness $\mathbf{u} - \mathbf{u}_m$ and the mode amplitudes are strictly not directly associated with one another. However, for the sake of simplicity we neglect the (small) difference due to the control function term $\gamma\mathbf{u}_c$, and define $e(\mathbf{y}, \gamma)$ as previously (equation (2.2)). The same derivation as described in section 2.1, but with the evolution equation constraint now given by the control function form

$$\frac{dy_i}{dt} = a_i + \sum_{j=1}^{N} b_{ij} y_j + \sum_{j=1}^{N} \sum_{k=1}^{N} c_{ijk} y_j y_k + d_i \frac{d\gamma}{dt} + (e_i + \sum_{j=1}^{N} f_{ij} y_j)\gamma + g_i \gamma^2 \tag{2.14}$$

yields

$$\delta E = \int_0^T [\frac{\partial e}{\partial \gamma} + \sum_{i=1}^{N} (e_i + \sum_{j=1}^{N} f_{ij} y_j + 2 g_i \gamma)\theta_i - \sum_{i=1}^{N} d_i \frac{d\theta_i}{dt}] \delta\gamma dt \tag{2.15}$$

Here the $\theta_i$ are defined by the requirements

$$\theta_i(T) = 0 \tag{2.16}$$

$$\frac{d\theta_i}{dt} = -\sum_{j=1}^{N} [b_{ji} + \sum_{k=1}^{N} (c_{jki} + c_{jik}) y_k + f_{ji}\gamma]\theta_j - \frac{\partial e}{\partial y_i} \tag{2.17}$$

and the additional condition

$$\delta\gamma(0) = 0 \tag{2.18}$$

is implied by the integration by parts leading to the $d\theta_i/dt$ term in equation (2.15). This condition is automatically satisfied by the parametrization equation (2.10) for $\gamma$, and the minimization algorithm proceeds as described in section 2.1, with

$$\delta\gamma_m = -\Delta_s \int_0^T [\frac{\partial e}{\partial \gamma} + \sum_{i=1}^{N} (e_i + \sum_{j=1}^{N} f_{ij} y_j + 2 g_i \gamma)\theta_i - \sum_{i=1}^{N} d_i \frac{d\theta_i}{dt}] sin(\frac{m\pi t}{2T}) dt \tag{2.19}$$

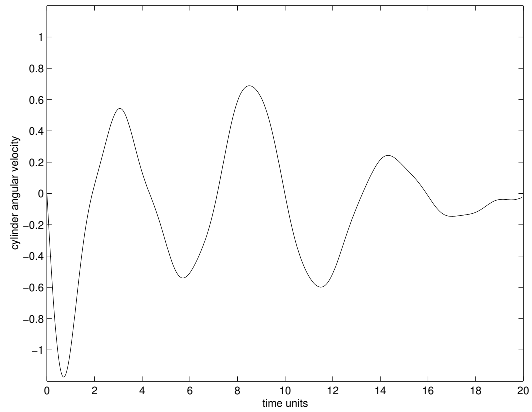


FIGURE 1. Optimized control action (control function method)

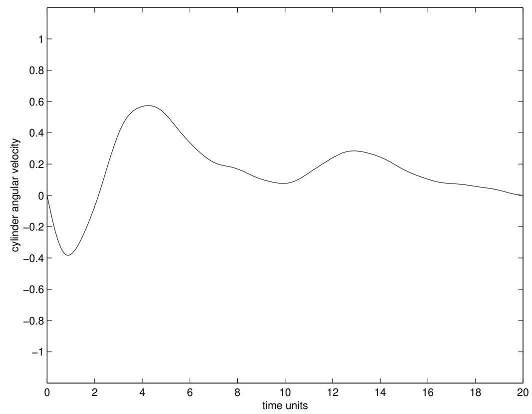


FIGURE 2. Optimized control action (penalty method)

This completes our specification of the optimal control formulations for the penalty and control function methods. We now compare their results for a sample test case.

## 2.3. *Optimal control test case*

For our test case, we take as initial condition the steady-state flow past the stationary cylinder, and derive the optimal control for a look-ahead time corresponding to about three vortex shedding periods ($T = 20$). The low order models used are those derived from the second generalized basis function set of Part I (generated from the unforced initial condition) and the forwards and backwards time integrations are carried out using a fourth-order Runge-Kutta method. The optimal control calculation is performed with $M = 50$ in the $\gamma$ parametrization (equation (2.10)), and is halted once the reduction in E is less than 5% of its current value. The constants governing the control expense, $C$ and $\gamma_{max}$ (see equation (2.2)) are taken to be 10 and 2 respectively.

The optimized control actions for the control function method and the penalty method are shown in Figures 1 and 2 respectively. In each case the prescribed rotation is clearly well bounded by our imposed limit $\pm\gamma_{max}$, and is largest over the first half of the time interval. This reflects the fact that later control action tends to affect mode amplitudes beyond the look-ahead time $T$ (due to delays associated with convection), and the optimal control thus sees no value in any effort here.

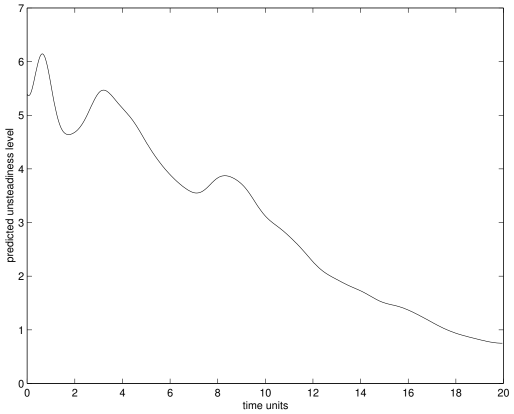


FIGURE 3. Unsteadiness history (control function method)

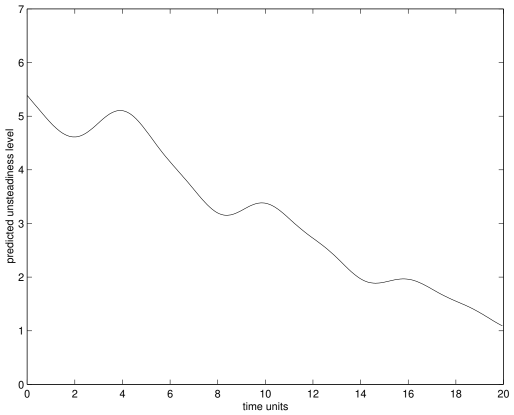


FIGURE 4. Unsteadiness history (penalty method)

The test of the algorithm lies in whether the control achieves its objective: minimization of the sum of the squared mode amplitudes. This quantity is plotted in Figure 3 and 4, from which it is clear that almost complete suppression is achieved by both approaches, in spite of the significant differences in the control actions.

This calculation is clearly optimistic, given the limited predictive ability of the low order model. However, one important feature of this example will carry over directly to the control of the simulation — the need to look ahead further than the time period for which a control prediction is required, so that the delayed effects of the control may be accounted for.

## 3. Optimal Control of the Cylinder Flow

In this section we discuss the application of the optimal control formulations to controlling the flow in the full Navier-Stokes simulation. Given the limited predictive capability of the low order models developed, some form of periodic re-initialization of the mode amplitude estimates, $y_i$, is necessary and here we assume this re-initialization to be performed with full knowledge of the flow field.

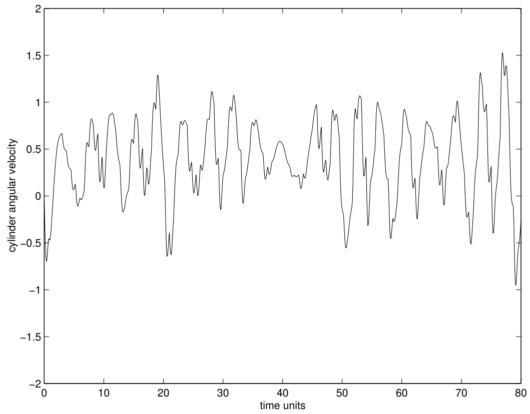


FIGURE 5. Optimized control action (control function method)

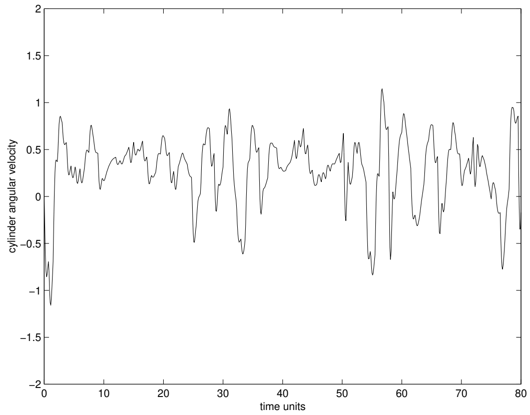


FIGURE 6. Optimized control action (penalty method)

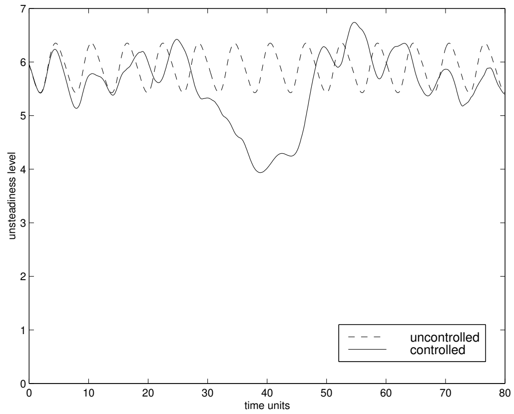


FIGURE 7. Unsteadiness history (control function method)

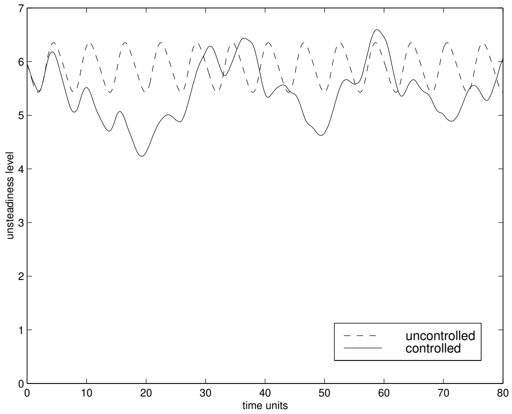


FIGURE 8. Unsteadiness history (penalty method)

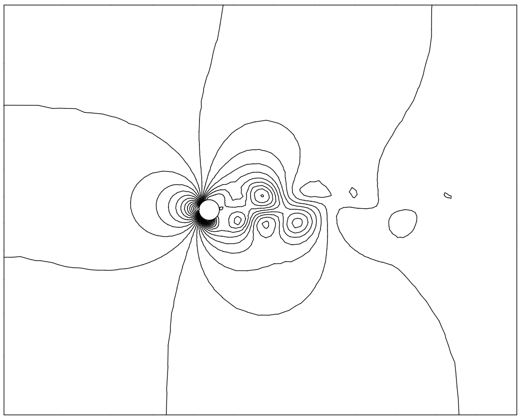

FIGURE 9. Pressure contour (control function method, $t = 40$)

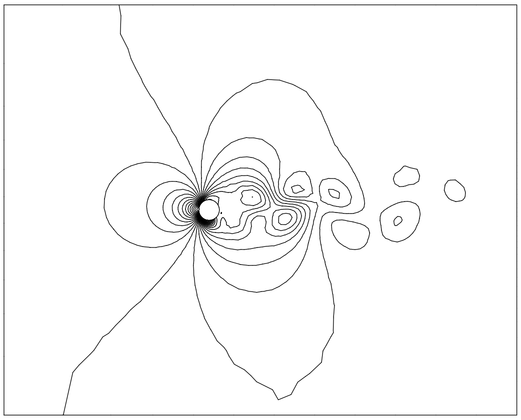

FIGURE 10. Pressure contour (penalty method, $t = 20$)

### 3.1. *Control of the Wake Unsteadiness*

We start by considering the control performance obtained with low order models derived from the unforced initial condition basis functions, using a reset time of 0.75 time units. An inspection of the open-loop results of Part I shows that little significant divergence between projection and prediction errors usually occurs within that period, and hence that the models should exhibit good accuracy if reset at this interval. However, as this is too short a time to see the effect of a control action on the wake unsteadiness, we specify a corresponding look-ahead time ($T$ in the formulation of section 2) of 10.0. Fifty design variables are used in the parameterization for $\gamma(t)$ and the values of $C$ and $\gamma_{max}$ are kept at 10 and 2 respectively. (Broadly similar results to those presented here are found if $M$ is reduced to 25, but further reduction degrades the control performance noticeably.)

The cylinder angular velocity time histories for the control function and penalty methods are plotted in Figures 5 and 6. The signals are qualitatively rather similar, notably in their positive bias, but (as in our previous test case) differ significantly in detail. The corresponding wake unsteadiness levels, shown in Figures 7 and 8, reflect the differences in control action. However, both show the desired reduction, at least in a time-averaged sense. The lowest unsteadiness level attained is around 4 in each case, but this appears only to be sustainable for a few time units. The unsteadiness then returns to around the uncontrolled value before starting to drop again.

The differences in the two controlled flows are emphasised by Figures 9 and 10, which show instantaneous pressure contours at the approximate point of lowest unsteadiness level ($t = 40$ for the control function method and $t = 20$ for the penalty method). The control function method appears to have virtually suppressed vortex shedding for a while, but it has subsequently been re-established. In contrast, the penalty method has achieved greater pressure attenuation, but has not suppressed shedding at any point in the visible history. In each case, the pressures are significantly lower than in the uncontrolled wake (Figure 3 of Part I), and the regular vortex street has been broken up into a less ordered pattern.

On the basis of these results, our single degree-of-freedom control has successfully achieved its aim: ie a reduction in the unsteadiness of the cylinder flow, without necessarily suppressing it entirely. Although the resulting unsteadiness levels are well above the predictions of section 2, they are below the uncontrolled value, and significantly below the levels which would be observed under arbitrary cylinder rotation.

### 3.2. *Model performance during control*

Further insight into the control simulations may be gained from the time histories of the error measures introduced in Part I. Figure 11 shows the projection and prediction errors for the control function method, along with the uncontrolled flow projection errors. The corresponding data for the penalty method are plotted in Figure 12. In each case, we observe that the projection error is higher when control is applied, and that the prediction error tends to grow more rapidly than in the open-loop test cases of Part I. The implication is that the flow tends to react to the control by moving away from the phase space spanned by the basis functions, thereby degrading the performance of the low order model. This places a further requirement for generality on the basis functions, and also raises important questions about the extent to which unsteady flows may be manipulated by simple control systems.

### 3.3. *Effect of varying reset time*

If the reset time is reduced, to 0.25 time units, the effectiveness of the control is improved, particularly at later times and more so for the penalty method. Increasing the reset time

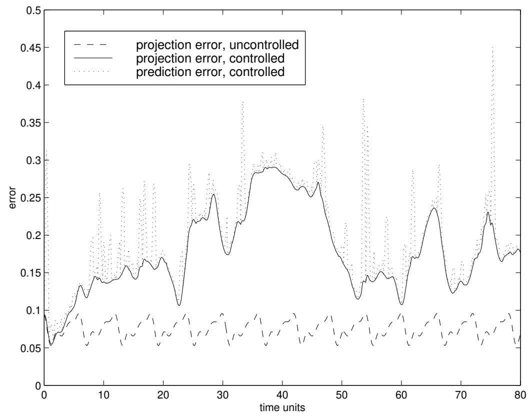


FIGURE 11. Error measures for control function method

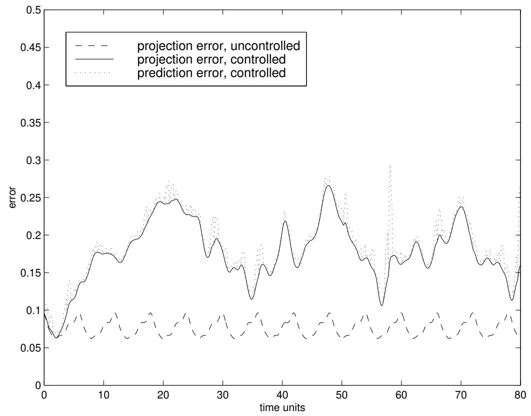


FIGURE 12. Error measures for penalty method

to 1.5 time units and beyond degrades the control function method results to the point where no clear difference between average controlled and uncontrolled unsteadiness levels is visible. The penalty method, however, still achieves reductions of the order of 10% for a reset time of 3.0 time units. Furthermore, these reductions are sustainable, and do not exhibit the returns to uncontrolled levels seen in Figures 7 and 8.

### 3.4. *Effect of the choice of basis functions*

In Part I a second set of basis functions, derived from the "chirp" excitation of an initially locked-on flow, was discussed. As a result of this initial condition (which has greater unsteadiness than the unforced shedding), these basis functions are less capable of describing the controlled flows, and may thus be expected to result in less effective control. Simulation results with the penalty method confirm this assumption, showing that unsteadiness levels actually tend to rise above uncontrolled values in this case.

## 4. Improving the Basis Function Set

The importance of the choice of basis functions to control performance suggests that consideration should be given to ways of improving the initial set. One approach might be to look for more appropriate open-loop excitations than the "chirp" used in Part I. However, when the error measures for the control simulations described here are inspected, two features stand out. Firstly, the projection errors for the controlled flows are higher than those for the uncontrolled flow (even taking into account the effect of reduced unsteadiness levels). Secondly, the rate at which the projection and prediction errors diverge when the flow is controlled is typically much greater than in the open-loop test cases. Taken together, these observations suggest that the flow tends to move away from the region of phase space spanned by the basis functions when control is applied, and that therefore refinements to the basis function set should be based on the controlled flow in some way. In this section we use penalty method simulation examples to discuss two possible approaches to this issue, on-line basis function augmentation (section 4.1), where additional basis functions are formed during the control simulation, and basis function regeneration (section 4.2), where a new basis set is created from the control simulation time history. Interestingly, we shall find that neither of these approaches yield all the benefits that one might naively expect, and the reasons for this are discussed in 4.3.

### 4.1. *On-Line Basis Function Augmentation*

This method is based on the observation that the difference between the simulated flow and the projection of this flow onto the basis functions is by definition orthogonal to all the existing basis functions. A new basis function may thus be generated simply by taking this difference and normalizing it suitably. Since the original basis functions are unchanged, only the coefficients involving the new member need be calculated in order to update the low order model, and the control simulation can then proceed from a condition with no error.

A convenient time to carry out this augmentation process is when the low order model is reset, and we additionally specify that the projection error should be above 10% in order to justify adding a basis function. The resulting controlled flow unsteadiness levels are compared with previous results in Figure 13. The augmentation approach clearly has a beneficial effect on the control, but the extent of the improvement is perhaps less than might be expected.

Some idea of the reasons for this may be gained from the projection and prediction errors during the simulation, shown in Figure 14. The notable feature of this plot is the rapid growth in the projection error frequently seen after each augmentation — much greater than is observed in the original control. The implication is that the instantaneous errors which we use to generate the additional basis functions are not necessarily representative of later flow fields, and thus tend to affect the model performance adversely. This conclusion is strengthened by inspecting individual basis function amplitudes, where the predictions for the additional functions tend to be much worse than those for the original set. After some time, however, the augmented basis function set consistently achieves projection errors below those of the uncontrolled flow (unlike the original control), and the control performance improves.

From this result, it is clear that on-line augmentation in this simple form is not an ideal way of improving our low order model. Since the reason for this appears to be the lack of general applicability of the additional functions, we next consider an approach which takes account of variations over time — basis function generation from snapshots of the controlled flow.

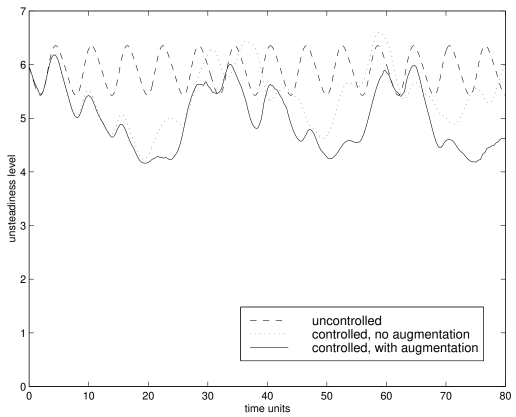


FIGURE 13. Effect of basis function augmentation on unsteadiness levels

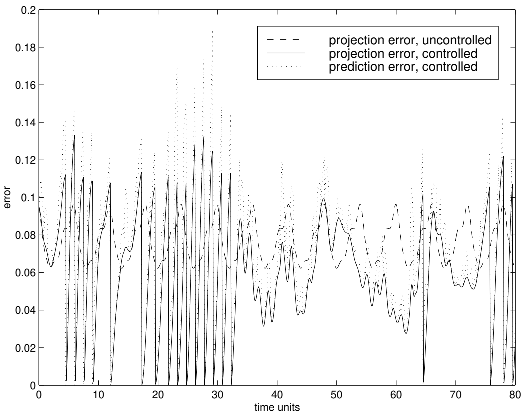


FIGURE 14. Error measures for control with basis function augmentation

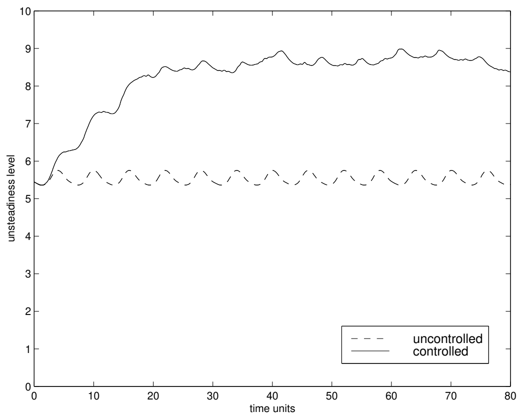


FIGURE 15. Unsteadiness history (penalty method, regenerated basis functions)

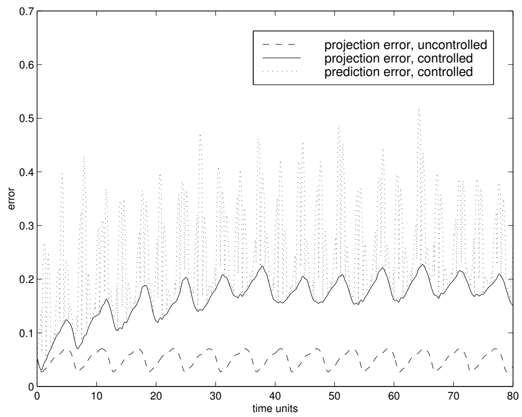


FIGURE 16. Error measures (penalty method, regenerated basis functions)

### 4.2. *Basis Function Regeneration*

For this method, we take snapshots from the original controlled flow of section 3 and generate a new set of basis functions, which may then be used to furnish a new low order model for use in the control simulation. For the results presented here 18 basis functions (capturing around 97% of the snapshot energy) were calculated from 75 snapshots taken every 0.64 time units.

The level of flow unsteadiness in the new controlled flow is plotted against time in Figure 15. Here we find that the "improved" basis function set yields markedly worse results than the original, increasing unsteadiness levels to around 9. The reasons for this behavior are evident in Figure 16, which shows that the projection error rapidly grows to around 20% for the controlled flow, even though the uncontrolled flow is well described by the new basis functions. The poor fidelity of the new model is further emphasised by the extremely rapid growth in prediction error after each reset. On a more detailed level, we find that the new basis functions have features similar to those found for steady state flows (Part I, section 3), in particular strong spatial correlation between conditions at the cylinder and far downstream. The associated weakness of the steady state low order models thus reappears here to some extent, with detrimental effects on the control.

### 4.3. *Discussion*

The results of section 4.1 and 4.2 clearly demonstrate that a basis function improvement strategy must be sophisticated if it is to succeed. Simply regenerating basis functions from snapshots of an initial control attempt leads to undesirable spatial correlation in the resulting low order model, while augmenting the basis function set using instantaneous errors can result in sub-optimal choices. Both of these problems may be thought of as arising from the overly "tuned" nature of the proposed approaches. We are thus faced with two conflicting requirements: the need to extend the basis function set in order to describe the new flow regimes found when control is applied, and the need to do so in a non-specific way. This is clearly an area requiring further work; however we note that one possibility would be to extend the on-line augmentation approach by taking error flow snapshots, and forming basis functions in the usual way from these data. In this way one would at least be sure of capturing the dominant structures in the previous error history, rather than an instantaneous estimate.

## 5. Optimal Control Based on Measurement Information

The control simulations presented in sections 3 and 4 make the unrealistic assumption that full knowledge of the flow field is available when the low order model is reset. Given that this idealized approach has been shown to be successful in reducing wake unsteadiness, it is now of interest to assess the control performance when limited flow information is provided. Here we take this information to be a small number of velocity measurement time histories, and use both the temporal and spatial resolution of the data to estimate basis function amplitudes. The theoretical background to this approach is developed in section 5.1, and the corresponding control simulation results are presented and discussed in sections 5.2 and 5.3 respectively.

### 5.1. *Optimal Estimation of Mode Amplitudes from Measurement Data*

We assume that we have a set of J velocity measurements $\mathbf{v}(\mathbf{x}_j, t) = \mathbf{u}(\mathbf{x}_j, t) - \mathbf{u}_m(\mathbf{x}_j)$, henceforth referred to as $\mathbf{v}_j$, and we wish to find the estimated basis function amplitudes $\hat{y}_i$ that minimize the error

$$E = \int_0^T \sum_{j=1}^{J} (\mathbf{v}_j - \sum_{i=1}^{N} \hat{y}_i \boldsymbol{\Psi}_{ij})^2 dt \tag{5.1}$$

(with $\boldsymbol{\Psi}_{ij} = \boldsymbol{\Psi}_i(\mathbf{x}_j)$), subject to the constraint imposed by our low order model. With the penalty method formulation (equation (2.3)) this is equivalent to minimizing

$$\begin{aligned} E = \int_0^T \sum_{j=1}^{J} (\mathbf{v}_j - \sum_{i=1}^{N} \hat{y}_i \boldsymbol{\Psi}_{ij})^2 dt - \int_0^T \sum_{i=1}^{N} \theta_i \Big( \frac{d\hat{y}_i}{dt} - a_i^p - \sum_{j=1}^{N} b_{ij}^p \hat{y}_j \\ - \sum_{j=1}^{N} \sum_{k=1}^{N} c_{ijk} \hat{y}_j \hat{y}_k - d_i^p \gamma \Big) dt \end{aligned} \tag{5.2}$$

where (as in section 2) the $\theta_i$ are adjoint functions, currently arbitrary, whose properties will be chosen to facilitate the calculation.

Given the $\mathbf{v}_j$ and $\gamma$, the variation in equation (5.2) is

$$\begin{aligned} \delta E = \int_0^T \sum_{i=1}^{N} \Big( \frac{d\theta_i}{dt} + \sum_{j=1}^{N} [b_{ji}^p + \sum_{k=1}^{N} (c_{jki} + c_{jik}) \hat{y}_k] \theta_j \\ -2 \sum_{j=1}^{J} \boldsymbol{\Psi}_{ij} \cdot (\mathbf{v}_j - \sum_{k=1}^{N} \hat{y}_k \boldsymbol{\Psi}_{kj}) \Big) \delta\hat{y}_i dt - \sum_{i=1}^{N} [\theta_i \delta\hat{y}_i]_0^T \end{aligned} \tag{5.3}$$

Thus, if the adjoint functions $\theta_i$ are chosen such that

$$\theta_i(T) = 0 \tag{5.4}$$

$$\frac{d\theta_i}{dt} = -\sum_{j=1}^{N} [b_{ji}^p + \sum_{k=1}^{N} (c_{jki} + c_{jik}) \hat{y}_k] \theta_j + 2 \sum_{j=1}^{J} \boldsymbol{\Psi}_{ij} \cdot (\mathbf{v}_j - \sum_{k=1}^{N} \hat{y}_k \boldsymbol{\Psi}_{kj}) \tag{5.5}$$

then $\delta E = \sum_{i=1}^{N} \theta_i(0) \delta\hat{y}_i(0)$, and the steepest descent choice

| Measurement no. | x coordinate | y coordinate |
|---|---|---|
| 1 | 8.0 | -1.0 |
| 2 | 1.0 | 0.3 |
| 3 | 12.7 | -0.4 |
| 4 | -0.2 | 0.5 |
| 5 | 1.6 | -0.9 |
| 6 | 5.0 | 0.2 |
| 7 | 9.0 | 1.0 |
| 8 | 11.1 | 0.1 |
| 9 | 2.3 | 1.3 |

TABLE 1. Measurement positions

$$\delta\hat{y}_i(0) = -\Delta_s\theta_i(0) \tag{5.6}$$

reduces the error, for sufficiently small $\Delta_s$. As previously, a line search is required to optimize $\Delta_s$, and a number of steepest descent steps will be required before convergence is achieved. For each step, the low order model is integrated forwards from initial conditions $\hat{y}_i(0)$, and the adjoint functions $\theta_i$ are then determined by backwards integration. This yields the steepest descent gradient and, after optimization of $\Delta_s$, equation (5.6) gives the new $\hat{y}_i(0)$. Once the process is converged, the desired current mode amplitude estimates are given by $\hat{y}_i(T)$. For the results presented here, convergence is defined by the error reduction for a step being less than 1% of the error before the step.

### 5.2. *Control Simulations*

The preceding analysis provides no guidance on the choice of measurement location positions, nor on their number. In principle, with enough time resolution and an accurate enough low order model, one location should suffice, but in practice several will be required. For these simulations, positions were chosen semi-heuristically. The first was selected on the basis of the amplitude of the coefficient vector, $\sum_i |\mathbf{\Psi}_{ij}|^2$, and the extent to which its component magnitudes $|\mathbf{\Psi}_{ij}|^2$ were of similar size. Subsequent potential locations were ranked by the extent to which their coefficient vectors were orthogonal to those already chosen ($\sum_i \mathbf{\Psi}_{ij}\mathbf{\Psi}_{ik} \cong 0$) and of large magnitude. The resulting measurement positions are given in Table 1.

Preliminary assessments of the optimal estimation algorithm were made using measurement time histories from the uncontrolled, unforced flow. For the low order model constraint to contribute significant information to the optimization process, a time interval of about 3 time units was found necessary ( over shorter times the system dynamics are not clearly apparent. With this time interval, the error in the final estimate $\hat{y}_i(T)$ was found to be approximately 15% when the first six measurements were used, and 10% when all nine were employed (this compared with an instantaneous projection error of 6.6%). Simulation results with six measurements proved unsatisfactory, so those presented here use nine. Other parameters are identical to those used for the penalty method example in section 3.

The resulting unsteadiness levels are plotted in Figure 17. Note that no control is applied during the first three time units, over which the initial mode amplitude estimation is performed. The use of estimated basis function amplitudes clearly degrades the control

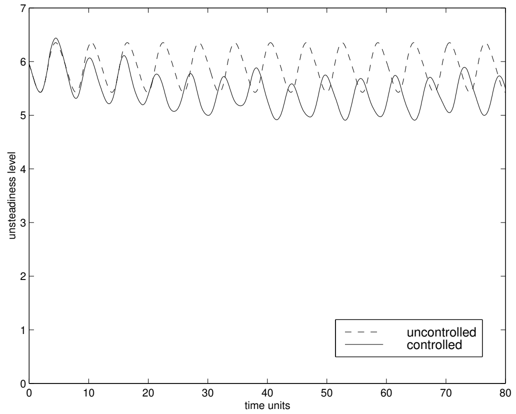


FIGURE 17. Unsteadiness history (penalty method, based on measurement information)

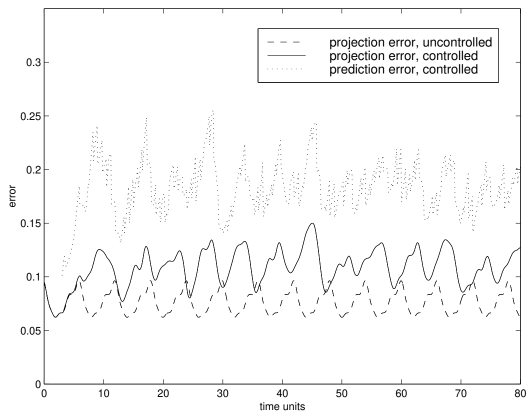


FIGURE 18. Error measures (penalty method, based on measurement information)

performance to some extent (compared with Figure 8); however it still proves possible to reduce wake unsteadiness levels consistently.

Error measures for this test case are plotted in Figure 18. The imperfect nature of the estimation process is reflected in the difference between the projection and prediction errors at the reset times, and this tends to increase the average error in the mode amplitudes. However, the optimal estimates are clearly successful in controlling the model inaccuracy, with the result that the control aims can still be attained.

Increasing the reset time for this case from 0.75 has broadly the same effect as described for the corresponding example in section 3. However, decreasing it to 0.25 no longer improves the control — in fact the unsteadiness rises significantly above uncontrolled levels after about 40 time units. This poor performance is found to be linked to high projection (and prediction) errors, indicating that the flow has moved away from the space spanned by the basis functions.

### 5.3. *Discussion*

The results of this section indicate that the control approach introduced in section 3 remains applicable even when supplied with only limited information. Inevitably, the optimal estimation procedure of equation (5.2) yields only approximate basis function amplitudes, but with nine measurements these prove sufficiently accurate to allow the control to function, albeit with somewhat degraded performance. Given the heuristic approach used in the choice of measurement positions, it is likely that better results, or similar results with fewer measurements, could be achieved by optimizing the locations. However, the main issue of interest, whether the low order model-based control can work successfully given limited information, is clearly answered by the data presented here. Note, however, that there now appears to be a limit to how strictly one can attempt to control the flow, the unsuccessful results for a reset time of 0.25 suggesting that it is possible to drive the flow into regions where the low order model is inaccurate and counter-productive.

## 6. Conclusions

In this paper we have presented investigations into the application of the low order models developed in Part I to control of the unsteadiness in the cylinder wake. Specifically, we have derived optimal control formulations for the penalty method and control function method low order models (section 2) and applied them to the numerical flow simulation (section 3), demonstrating that it is possible to reduce the wake unsteadiness via this approach, as long as one can reset the model periodically. However, a poor choice of basis functions for the low order model can negate the benefits of the control, and even cause the unsteadiness to rise.

The importance of the basis functions to the control performance automatically leads to consideration of ways to improve an initial set. Here, we have investigated two natural approaches to this problem — on-line basis function augmentation and basis function regeneration (section 4). However, both these methods (in particular the regeneration approach) have been found to produce mixed results, due to their tendency to yield models which are too highly "tuned". This issue thus remains open, although the more generalized on-line augmentation proposed in section 4.3 may well represent an acceptable solution.

Lastly, we have developed a method for estimating basis function amplitudes closely linked to the optimal control ideas of section 2, and have applied this approach to measurement-based control of the flow (section 5). Although there is some degradation in performance compared to the idealized, perfect reset, results presented in section 3, we have shown that the control aims are achievable, given a limited number of measurements.

We conclude, then, that low order model-based control of this flow is possible, and that the level of unsteadiness in the cylinder wake can be reduced. However the complexity of our control "system" is markedly greater than would originally be suggested from a consideration of the uncontrolled flow, and this leads us to the general conclusion that actively-controlled flows may, in general, exhibit many more significant degrees of freedom than their unforced counterparts. Furthermore, attempts to control the degrees of freedom participating at a given time may tend to push the flow into other regions of phase space, and the low order model employed must be capable of describing these regions sufficiently well to enable successful control. Here we have achieved best results with basis functions generated by a varying frequency "chirp" in the cylinder rotation rate, starting from an unforced flow initial condition. The resulting low order model has been shown to be capable of describing the range of wake flows encountered with reasonable fidelity. Attempts to refine the model have only been successful if they have not affected this non-specific nature.

This discussion raises the question of whether it is possible to have a low order model which describes the controlled flow to a high degree of accuracy, or whether attempts to generate such a model and apply it to control the flow will simply excite more and more degrees of freedom. It is highly unlikely that our most successful model here is the best possible one; however one can conjecture that one should not try and control this flow too "rigorously" and that hence one should not seek the "perfect" model.

Lastly, we observe that the unsteady lift on the cylinder may well be more amenable to control via rotation than the wake unsteadiness. Model-based control of this quantity requires some means of estimating the pressure field in the flow, which, in principle, is completely determined by the instantaneous velocity field and the boundary conditions. Using this fact, it is possible to derive a set of coefficients giving the linear and quadratic contributions to $C_L$ from the mode amplitudes and hence to define an appropriate cost function. Control simulations with perfect model reinitialization have been performed, with promising results, but the approach to calculating $C_L$ described here proves to be very sensitive to errors in the mode amplitudes and measurement-based control has therefore not been attempted. For effective lift coefficient control, it is likely that a different pressure calculation technique will be required. A potential candidate here is a separate low order model, with appropriate basis functions, "driven" by the velocity basis function amplitudes.

## Acknowledgments

The authors wish to express their gratitude to Jim Paduano, Kenny Breuer, Eric Feron and Stuart Jacobson for their contributions to a number of helpful discussions.

## REFERENCES

Lions, J. L. 1971 *Optimal Control of Systems Governed by Partial Differential Equations.* Springer-Verlag, New York.

Pironneau, O. 1984 *Optimal Shape Design for Elliptic Systems.* Springer-Verlag, New York.